# Preparation of nanophase M-type ferrite and its laser-attenuated characteristics

**LIU Xiang-cui**(刘香翠)*, **CHENG Xiang**(程翔), **ZHANG Liang**(张良), **LIU Jian-hui**(刘建辉), **and DU Gui-ping**(杜桂萍)

*Research Institute of Chemical Defense, Beijing 102205, China*

(Received 8 April 2011)



By citrate sol-gel auto-combustion method, the nanophase M-type planar hexagonal ferrite is prepared. The transmission electron microscopy (TEM), X-ray diffraction (XRD) and thermal analysis are used to study the grain size, phase composition, microstructure and crystallization process. The results show that the nanophase M-type Sr-ferrite prepared by this method is single, and its grain size is smaller than 100 nm. Moreover, most of the grains present hexagonal sheet shape. Tests are carried out for its attenuation to 1.06 μm laser. It is found that the extinction capability of the nanophase M-type Sr-ferrite smoke is good, and its mass extinction coefficient is 1.628 $m^2/g$.

**Document code:** A **Article ID:** 1673-1905(2011)04-0287-4

**DOI** 10.1007/s11801-011-1028-5

In recent years, with the latest development in radar and microwave communication technology, the new and efficient electromagnetic wave absorbing materials have become a focus and attracted more interests around the world[1-4]. The hexagonal ferrite, a main radar absorbing material, has been widely used at home and abroad[5-11] because of its strong absorbing ability, broad-band absorbency and low-cost preparation. But the bigger particle size and specific gravity by traditional preparation methods can't fulfill the strategic requirements of future applications for radar absorbing materials. Therefore, preparation and application of nanophase hexagonal ferrite are turning into the research focuses now[12-14].

In this paper, the nanophase M-type planar hexagonal Sr-ferrite is prepared by means of citrate sol-gel auto-combustion method. Its performance, including grain size, phase composition, microstructure and crystallization process, is characterized. Moreover, as a new smoke material, its attenuation performance to 1.06 μm laser is tested in a 20 $m^3$ smoke chamber.

The nanophase M-type $SrFe_{12}O_{19}$ is synthesized by citrate sol-gel auto-combustion process as follows. Analytically pure strontium nitrate, iron nitrate and citric acid are selected as raw materials. Firstly, strontium nitrate and iron nitrate in stoichiometric proportion are added to proper amount water solution of citric acid. With stirring, the mixed system in water bath is heated at 80 °C till the insoluble matters are dissolved completely. Secondly, adjust pH to about 7 using ammonia and keep on stirring for 2 h at 80 °C in water bath. Then the mixed solution is moved into the oven where it is dried in 130 °C till dark brown brittle xerogel is formed. As soon as the xerogel is ignited at a certain condition, the combustion can spread out rapidly and stably, as far as the xerogel is burned away to make fluffy powder. Then the powder is moved into the muffle furnace where it is presintered for 2 h at 450 °C and is sintered for 4 h at 900 °C. Lastly, after natural cooling, the brown-red Sr-ferrite powder is gained.

In this paper, main complex reactions are:

$$\begin{array}{l} CH_2COOH \\ C(OH)COOH+2NH_4OH \\ CH_2COOH \end{array} \rightarrow \begin{array}{l} CH_2COONH_4 \\ C(OH)COOH \\ CH_2COONH_3 \end{array} + 2H_2O, \quad (1)$$

$$\begin{array}{l} CH_2COONH_4 \\ C(OH)COOH + Sr^{2+} \\ CH_2COONH_4 \end{array} \longrightarrow \begin{array}{l} CH_2COONH_3 \\ C(OH)COOH\ Sr \\ CH_2COONH_3 \end{array} + 2H^+, \quad (2)$$

$$3\begin{array}{l} CH_2COONH_4 \\ C(OH)COOH + 2Fe^{3+} \\ CH_2COONH_4 \end{array} \longrightarrow Fe_2(C_6H_6O_7(NH_3)_2)_3 + 6H^+. \quad (3)$$

Citric acid is a complexing reagent and can complex with some metallic ions. Solid state reaction of metal complex occurs at high temperature, which produces nanophase M-type hexagonal $SrFe_{12}O_{19}$.

The phase composition of brown-red $SrFe_{12}O_{19}$ powder is analyzed by means of XD-D1 X-ray diffractometer pro-

* E-mail: liuxiangcui2001@yahoo.com.cn

duced by Shimazu (Cu diffraction target, target voltage of 20 kV, target current of 35 mA, scanning speed of 10°/min and scanning range of 20°−80°). On the other hand, its topography and particle size are observed by the transmitted electron microscope (H-700, Hitachi, Japan). And the crystallization process of xerogel is studied by thermal analyzer (heating rate of 10 °C/min and air flow rate of 20 mL/min).

The transmission electron microscope (TEM) image of the sample, magnified to 48 thousand times, is shown in Fig.1. From that, the particle size of the sample is 40−70 nm and its crystal grain is regular planar hexagonal sheet, which is the optimum shape of absorbing materials[12,15-17].

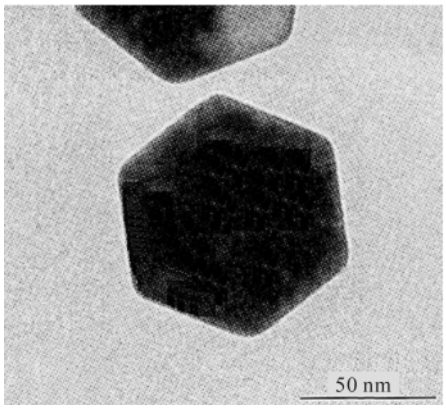


**Fig.1 TEM image of the $SrFe_{12}O_{19}$ sample**

The XRD pattern of $SrFe_{12}O_{19}$ sample is shown in Fig.2. Compared with the standard pattern of M-type $SrFe_{12}O_{19}$, diffraction peaks of the sample basically agree with the standard diffraction peaks. Consequently, the main production of the sample is M-type $SrFe_{12}O_{19}$.

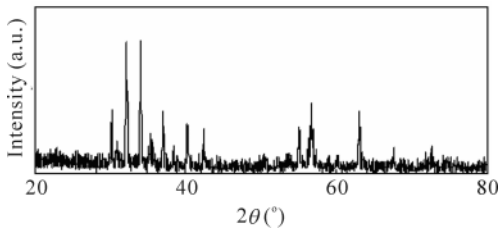


**Fig.2 XRD pattern of the $SrFe_{12}O_{19}$ sample**

Furthermore, the grain size of sample can also be determined according to Scherer formula[18]:

$$B_{2\theta} = \frac{K\lambda}{D\cos\theta} \quad , \tag{4}$$

where $B_{2\theta}$ is the half height of diffraction peaks, $K$ is approaching a constant 0.89, $\lambda$ is X-ray wavelength, $D$ is the average diameter of crystal grain, and $\theta$ is the angle of diffraction peak.

By means of Eq.(4), $D$ is given by:

$$D = \frac{K\lambda}{B_{2\theta}\cos\theta} \quad , \tag{5}$$

from which the average diameter of crystal grains is 63.3 nm, which is consistent with the analytical results of TEM.

Thermogravimetric (TG) and differential scanning calorimeter (DSC) curves of xerogel are shown in Fig.3 and Fig.4, respectively. The data obtained reveals its crystallization process. At 220 °C, an acute and narrow exothermic peak occurs in DSC curve. Simultaneously, the violent weight loss appears from TG data. It shows that at this temperature, main thermal reactions occur with great quantity of released heat and rapid reaction rate. It can be thought that the xerogel can spontaneously combust under the condition of thermal excitation. At the same time, the oxygen can accelerate the process of combustion. Accordingly, at 220 °C, the nitrate can produce autocatalytic redox reaction with carbonaceous groups of xerogel, which results in the nitrate decomposing. From Fig.4, the exothermic peak at 350−450 °C is caused by the decomposition of nitrate of xerogel. In this temperature range, the xerogel is predecomposed to ultrafine $\gamma$-$Fe_2O_3$ and $SrCO_3$, and obvious weight loss also occurs in TG curve. After 750 °C (crystals have formed completely), no apparent exothermic peak appears in DSC curve and the TG curve is flat, which means that main chemical reactions have already been accomplished. Combined with XRD pattern, it can be educed that the single uniform M-type Sr-ferrite has been produced since 750 °C.

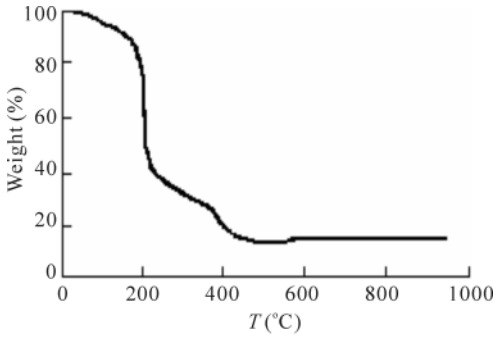


**Fig.3 TG curve of xerogel**

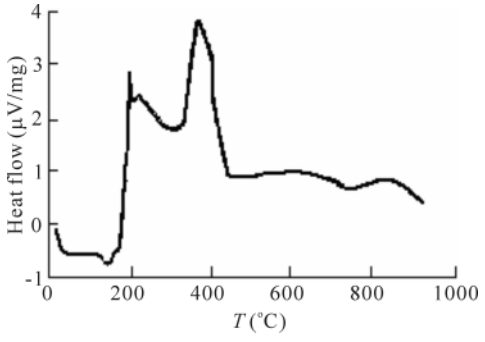


**Fig.4 DSC curve of xerogel**

Furthermore, the attenuation performance to 1.06 μm laser of nanophase M-type Sr-ferrite is tested in a smoke chamber which is 6.1 m×2.0 m × 1.8 m and its effective volume is 20 $m^3$, including spraying, stirring and sampling equipments (see Fig.5). The output wavelength of laser testing system is 1.06 μm. Transmittance is tested and displayed per second by the signal control system. After the emitter and the receiver of laser are adjusted, the transmittance of background is obtained. 30 g nanophase Sr-ferrite sample is sprayed into the smoke chamber by the spray nozzle with high-pressure air. At the same time, two mixing fans are operated continuously for 20 s at low speed to maintain uniform concentration. After the laser signal passes the smoke, its power data is collected. The sampling devices work to make smoke concentration measurements at a flow rate of 40 L/min. In the end, open the door of smoke chamber and start up the exhaust set to exhaust the remainded smoke particles in the chamber.

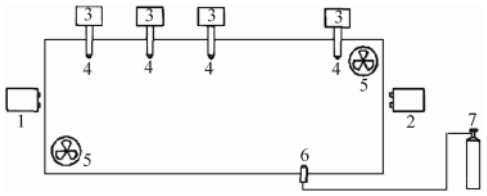


**Fig.5 Sketch of smoke chamber**

1, 2-laser testing system; 3-air pump; 4-sampling head of mass concentration; 5-mixing fan; 6-spray nozzle; 7-air compressor

The transmittance to 1.06 μm laser for 30 g nanophase M-type Sr-ferrite sprayed into the smoke chamber is shown in Fig.6. It can be seen that the transmittance drops sharply and reaches the minimum of less than 1% rapidly after the spraying of sample. It indicates that as the time is going by, the transmittance to 1.06 μm laser increases slowly and smoothly.

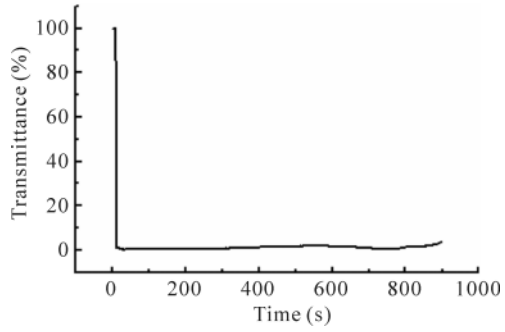


**Fig.6 Transmittance of nanophase M-type Sr-ferrite sample to 1.06 μm laser**

The mass extinction coefficient $\alpha$ is one of the most important performance parameters that are used to judge the attenuation performance of a material. The bigger $\alpha$ ($m^2/g$) is, the better its attenuation effect on the laser radiation is. According to Lambert-Beer law[19], the transmittance $T$ is calculated by:

$$T = I / I_0 = \exp(-\alpha C_m L) , \quad (6)$$

where $I_0$ is the intensity of laser incident radiation, $I$ is the transmitted intensity, $C_m$ is the mass concentration of material ($g/m^3$), and $L$ ($L$=6.1 m) is the length of the chamber.

Eq.(6) shows that $T$ depends on $\alpha$ if the concentration and thickness of smoke are invariable. By means of Eq.(6), $\alpha$ is given by:

$$\alpha = \frac{1}{C_m L} \ln \frac{1}{T} . \quad (7)$$

By pumping a certain volume of smoke, smoke particles are collected onto glass fiber filters that have been weighed. In Eq.(7), the mass concentration $C_m$ is calculated by means of

$$C_m = \frac{w - w_1}{v} = \frac{w - w_1}{Q \cdot t} , \quad (8)$$

where $w_1$ is the pure filter mass, $w$ is the filter mass after catching smoke particles, $v$ is the pumped smoke volume, $Q$ is the flow rate of rotometer (40 L/min), and $t$ is the sampling time (1 min).

Drawing on Eq.(8), the average $C_m$ of smoke in different time is computed, and the average transmittance in sampling intervals is got, which is used in Eq.(7) to obtain the mass extinction coefficients in different intervals, as shown in Tab.1. From Tab.1, the mass extinction coefficient of nanophase M-type Sr-ferrite to 1.06 μm laser is 1.628 $m^2/g$, which is higher than that of some conventional smoke compositions in Ref. [20] (as shown in Tab.2). This is because it has a smaller particle size and larger specific surface area which is over a thousand times greater than that of powders commercially available[21,22]. Excessive atoms and chemical bonds in its surface increase the interfacial activity. Consequently, the nanophase M-type Sr-ferrite exhibits good extinction characteristic to 1.06 μm laser.

**Tab.1 Mass extinction coefficient of nanophase M-type Sr-ferrite sample to 1.06 μm laser**

| Time (min) | $C_m$($g/m^3$) | $T$(%) | $\alpha$($m^2/g$) | $\bar{\alpha}$($m^2/g$) |
|---|---|---|---|---|
| 1-2 | 0.741 | 0.056 | 1.657 | 1.628 |
| 4-5 | 0.475 | 0.973 | 1.599 | |

**Tab.2 Mass extinction coefficient of some conventional smoke compositions to 1.06 μm laser in Ref.[20]**

| Code for material | 1 | 2 | 4 | 5 | 7 |
|---|---|---|---|---|---|
| $\alpha$($m^2/g$) | 1.04 | 1.17 | 1.09 | 1.16 | 1.50 |

In conclusion, the nanophase M-type planar hexagonal Sr-ferrite is prepared by means of citrate sol-gel auto-combustion method. The testing results of TEM, XRD, TG and DSC show that the M-type Sr-ferrite nano-powder prepared by this method is single. Its particle size is smaller than 100 nm and its crystal grain is regular planar hexagonal sheet. Furthermore, the testing results of attenuation performance show that as a new smoke obscurant material, it has good extinction capability to 1.06 μm laser.

## References


[1] Zhang X F, Dong X L, Huang H, Lv B, Lei J P and Choi C J, Journal of Physics D: Applied Physics **40**, 5383 (2007).

[2] Wu K H, Ting T H, Wang G P, Ho W D and Shih C C, Polymer Degradation and Stability **93**, 483 (2008).

[3] Liu J R, Itoh M, Horikawa T, Kuwano N and Machida K, Journal of Applied Physics **37**, 2737 (2004).

[4] Zhang Lan and Zhu Hong, Materials Letters **63**, 272 (2009).

[5] Wang L X and Zhang Q T, Journal of Alloys and Compounds **469**, 251 (2009).

[6] Qiu J, Wang Y and Gu M, Materials Letters **60**, 2728 (2006).

[7] Shams M H, Salehi S M A and Ghasemi A, Materials Letters **62**, 1731 (2008).

[8] Chen Yu-wei, Deng Min and Xiong Guo-xuan, Bulletin of the Chinese Ceramic Society **28**, 973 (2009). (in Chinese)

[9] Ghasemi A, Hossienpour A, Morisako A, Saatchi A and Salehi M, Journal of Magnetism and Magnetic Materials **302**, 429 (2006).

[10] Huang Xiao-gu, Chen Jiao, Wang Li-xi, Song Jie, Xu Nai-cen and Zhang Qi-tu, Electronic Components and Materials **29**, 54 (2010). (in Chinese)

[11] Yan Xin, Hu Xiao-ling, Yue Hong, Zhang Qiu-yu, Huang Ying and Lu Ling, Materials Review **15**, 62 (2001). (in Chinese)

[12] Tan Hong-bin and Ma Xiao-ling, Journal of Ceramics **29**, 77 (2008). (in Chinese)

[13] Bregar V B, IEEE Transactions on Magnetics **40**, 1679 (2004).

[14] Ren Hui, Jiao Qing-jie, Kang Fei-yu, Cui Qing-zhong and Li Jiang-cun, Rare Metal Materials and Engineering **36**, 223 (2007). (in Chinese)

[15] Yang Kai-xin, Journal of Magnetic Materials and Devices **27**, 19 (1996). (in Chinese)

[16] Wang Hai-bin, Liu Shu-xin, Huo Ji-chuan and Lv Shu-zhen, Bulletin of the Chinese Ceramic Society **27**, 754 (2008). (in Chinese)

[17] Li Bao-dong, Li Qiao-ling, Zhang Cun-rui and Zhao Jing-xian, Materials Review **22**, 226 (2008). (in Chinese)

[18] Editorial Committee of Chemical Encyclopedia, Editorial Department of Chemical Encyclopedia of Chemical Industry Press, Chemical Encyclopedia, Beijing: Chemical Industry Press, 1163 (1998). (in Chinese)

[19] Pan Gong-pei and Yang Shuo, Principles of Pyrotechnics, Beijing: Beijing Institute of Technology Press, 126 (1997). (in Chinese)

[20] Ren Li-na, Liu Hai-feng and Chen Liang, Infrared Technology **29**, 638 (2007). (in Chinese)

[21] Xu Bing-she, Nanometer Materials and Application Technology, Beijing: Chemical Industry Press, 14 (2003). (in Chinese)

[22] Zhang Li-de and Mu Ji-mei, Nanostructured Materials, Beijing: Science Press, 61 (2001). (in Chinese)